



Expression of Epstein-Barr virus-encoded BamH1-a rightward transcript 7 microRNA in nasopharyngeal carcinoma cells modulates the responsiveness to irradiation treatment

YWJ Chan[†], W Gao[†], ZHJ Li, WK Ho, TS Wong^{*†}

Abstract

Introduction

Nasopharyngeal carcinoma is highly sensitive to irradiation treatment. Expression of Epstein-Barr virus gene products affects the radiosensitivity of these cancer cells. In this paper, the association between the Epstein-Barr virus-encoded BamH1-a rightward transcript 7 microRNA (ebv-miR-BART7) and the effects on irradiation sensitivity was explored.

Methods

Ebv-miR-BART7 expression level in the tissue was quantified using real-time quantitative polymerase chain reaction. The radiosensitivity of nasopharyngeal carcinoma cells with ebv-miR-BART7 expression was evaluated by colony formation assay, cell proliferation assay, apoptosis assay, H2AX phosphorylation staining and acridine orange staining. In addition, a xenograft model was developed using a zebrafish embryo to validate the *in vivo* radiation sensitivity of the ebv-miR-BART7-expressing nasopharyngeal carcinoma.

Results

Primary and recurrent nasopharyngeal carcinoma tissues had a significantly higher ebv-miR-BART7 expression level in comparison with their corresponding normal counterparts. The ebv-miR-BART7-expressing nasopharyngeal carcinoma cells

had higher sensitivity to irradiation treatment.

Conclusion

Our results suggest that patients with nasopharyngeal carcinoma have elevated ebv-miR-BART7 expression levels in the primary and recurrent nasopharyngeal carcinoma tissues. Higher expression of ebv-miR-BART7 increased the sensitivity of nasopharyngeal carcinoma cells to irradiation treatment. Further investigation with regard to the clinical value of ebv-miR-BART7 to aid therapeutic response is warranted in order to evaluate the potential use of ebv-miR-BART7 as a molecular biomarker in monitoring patients with nasopharyngeal carcinoma.

Introduction

Nasopharyngeal carcinoma (NPC) commonly arises from the pharyngeal recess, the fossa of Rosenmüller, which is situated medial to the medial crus of the Eustachian tube opening into the nasal cavity¹. This cancer can originate from the epithelium overlying the lymphoid tissues and is also known as lymphoepithelioma or lymphoepithelial carcinoma². According to the World Health Organization classification, NPC can be classified into the following subtypes: squamous cell carcinoma (SCC, type 1, with different degrees of differentiation) and undifferentiated/non-keratinising carcinoma (type 2 and type 3), with variable response to therapeutic agents³. In comparison to SCC, early undifferentiated/non-keratinising carcinoma is more sensitive to irradiation treatment, and patients show an improved local

control rate in response to radiotherapy⁴. Thus, most of the early NPC patients are treated with irradiation-based therapy⁵. If the cancers acquire resistance during the course of treatment or are intrinsically resistant to irradiation treatment, it may lead to the development of local recurrence and distant metastasis⁶. At present, the reasons or the mechanisms leading to the high sensitivity and/or resistance of NPC to irradiation treatment remains unknown. It has been suggested that the sensitivity/resistance of cancer cells to irradiation treatment is affected by different apoptotic pathways associated with treatment response⁷.

Unlike SCC, undifferentiated/non-keratinising NPC is characterised by its close association with the Epstein-Barr virus (EBV), the first tumour virus found in association with human malignancies. EBV infection is specific to the tumour tissue and is absent in the adjacent normal nasopharyngeal epithelia. Recently, it was found that the EBV could produce a group of non-coding RNAs known as microRNAs (miRNAs) in the host cells⁸. These small, non-protein-coding RNAs (single-stranded) function as gene-specific regulators. Mature miRNAs can form a functional unit similar to the RNA-induced silencing complex used for RNA interference in the cytoplasm⁹. Functionally, miRNAs can regulate protein expression at the post-transcriptional level through direct binding to specific messenger RNA molecules. The specific binding of miRNA molecules can promote degradation of the messenger RNA and/or hinder the translation process. At present, little

* Corresponding author
Email: thiansze@graduate.hku.hk

[†] These authors contributed equally to this study.
Department of Surgery, The University of Hong Kong, Hong Kong

Licensee OA Publishing London 2013. Creative Commons Attribution Licence (CC-BY)

FOR CITATION PURPOSES: Chan YWJ, Gao W, Li ZHJ, Ho WK, Wong TS. Expression of Epstein-Barr virus-encoded BamH1-a rightward transcript 7 microRNA in nasopharyngeal carcinoma cells modulates the responsiveness to irradiation treatment. *Head Neck Oncol.* 2013 Mar 06;5(3):34.



is known about the functional role of the viral miRNA. Expression of the viral miRNA is suggested to be associated with the activity and replication of EBV⁸. In EBV-positive cell lines, high expression of EBV miRNA has been reported. Mature viral miRNAs can be detected in two days after infection and are regarded as an important initiator of the viral life cycle in host cells⁸. In addition, expression of the EBV-encoded miRNA can change the responsiveness of the NPC cells to DNA-damaging agents and modulate apoptosis signalling pathways^{10,11}.

In this paper, we explored the potential association between the

EBV-encoded miRNA (ebv-miR-BART7) and the responsiveness to irradiation treatment. The radiosensitivity of the NPC cells with ebv-miR-BART7 expression was examined with the use of *in vitro* cell irradiation. In addition, xenograft models were developed with the use of zebrafish embryos to examine these effects in the *in vivo* setting.

Materials and methods

Patient samples

Undifferentiated NPC tissue samples were obtained from the Department of Surgery, The University of Hong Kong, Queen Mary Hospital,

Hong Kong. Written consent of tissue donation for research purposes were obtained from patients before tissue collection. The protocol was approved by the Institutional Review Board of the hospital (reference number UW 10-142). Tissue samples were stored in liquid nitrogen for transportation and stored at -70°C until used. Tissue samples were collected from 42 patients with primary NPC, 29 with recurrent NPC and 29 non-cancer volunteers. The 42 patients with primary NPC included 32 males and 10 females, with age ranging from 12–75 years. There were 11 patients in the T1 stage, 9 in the T2 stage, 18

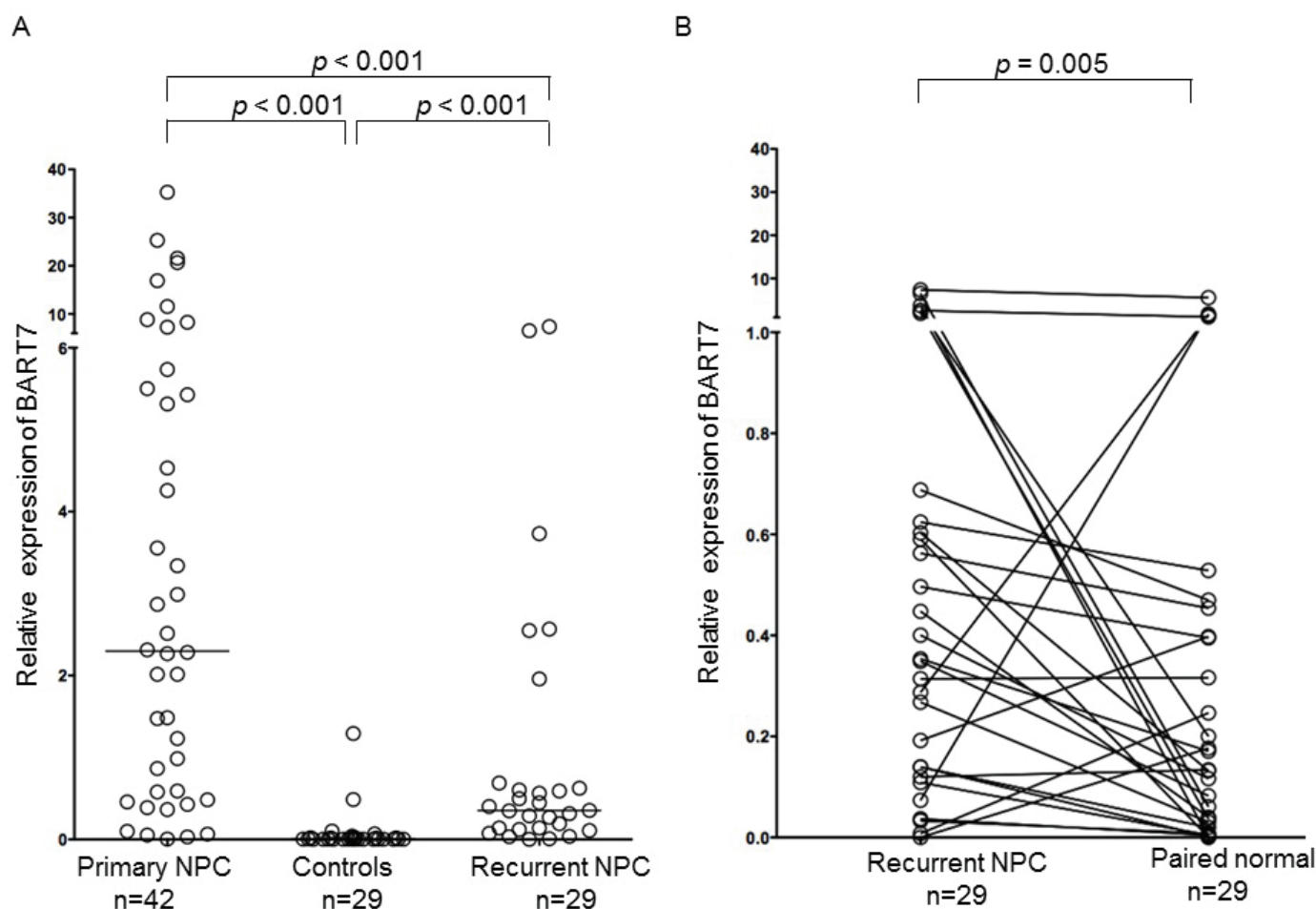


Figure 1: Relative ebv-miR-BART7 expression levels in tissue samples from patients with NPC and healthy controls. The relative expression level of ebv-miR-BART7 was normalised to U6 snRNA by quantitative polymerase chain reaction analysis and the data are displayed as $2^{-\Delta\text{Ct}}$. (A) Relative ebv-miR-BART7 expression levels in tissue samples from patients with primary NPC, recurrent NPC and healthy controls. (B) Relative ebv-miR-BART7 expression levels in paired tumour and normal samples from patients with recurrent NPC. NPC, nasopharyngeal carcinoma.

Licensee OA Publishing London 2013. Creative Commons Attribution Licence (CC-BY)

FOR CITATION PURPOSES: Chan YWJ, Gao W, Li ZHJ, Ho WK, Wong TS. Expression of Epstein-Barr virus-encoded BamH1-a rightward transcript 7 microRNA in nasopharyngeal carcinoma cells modulates the responsiveness to irradiation treatment. *Head Neck Oncol.* 2013 Mar 06;5(3):34.

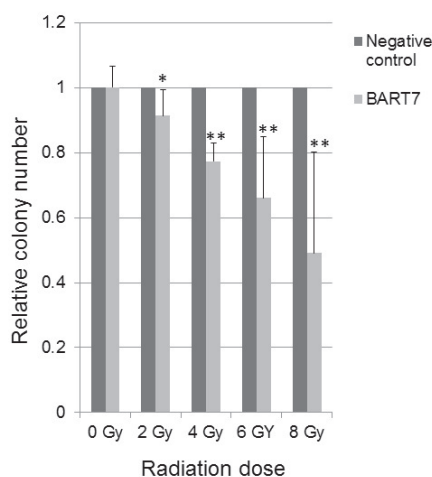


Figure 2: Ebv-miR-BART7 reduced colony formation ability in HONE1 cells after irradiation treatment. HONE1 cells were transfected with 3 nM ebv-miR-BART7 mimics or the negative control. After 24 hours, cells were irradiated at a single dose of 2, 4, 6 or 8 Gy. Following irradiation, cells were plated as 600 cells per well in a six-well plate and incubated for 14 days. Colonies consisting of more than 50 cells were scored. The number of colonies of HONE1 cells transfected with BART7 mimics was normalised to that of HONE1 cells transfected with the negative control. The assay was performed in six-replicate. Bars indicate standard deviation, * $p < 0.05$ and ** $p < 0.01$ by Student's t-test.

in the T3 stage and 4 in the T4 stage. The 29 patients with recurrent NPC included 22 males and 7 females, with age ranging from 29–75 years. There were 13 patients in the T1 stage, 4 in the T2 stage, 9 in the T3 stage and 3 in the T4 stage. The 29 healthy volunteers included 20 males and 9 females, with age ranging from 6–81 years.

Cell line

The NPC cell line HONE1 was derived from poorly differentiated NPC tissues. The EBV genome in the HONE1 cell line was lost after prolonged culture and passage¹². The cell line was maintained in an RPMI 1640 medium (Gibco®) supplemented with 10% foetal bovine serum (Gibco®), 200 unit/ml penicillin G sodium (Gibco®), 200 µg/ml

ml streptomycin sulphate (Gibco®) and 0.5 µg/ml amphotericin B; cells were incubated at 37°C in a humidified incubator under 5% CO₂.

RNA extraction and real-time quantitative polymerase chain reaction analysis

Total RNA was extracted with TRIZOL (Life Technologies™) following the manufacturer's protocol. The transcript levels of ebv-miR-BART7 (Assay ID: 197206_mat, Life Technologies™) and U6 small nuclear RNA (internal control, assay ID: 001973, Life Technologies™) were measured by LightCycler® 480 (Roche Applied Science) using the comparative cycle threshold method. All reactions were carried out in triplicate.

Cell irradiation

Cell irradiation was performed using Gammacell® 3000 Elansystem (Best Theratronics Ltd.).

Colony formation assay

HONE1 was transfected with 3 nM ebv-miR-BART7 mimics (Qiagen) or negative control small interfering RNA (siRNA, Qiagen) using Hiperfect transfection reagent (Qiagen). After 24 hours, the cells were transferred to a fresh medium and were irradiated at a single dose of 2, 4, 6 or 8 Gy. The irradiated cells were placed in a six-well plate (600 cells per well) and incubated for 14 days. The cells were fixed with 70% ethanol and stained with 0.5% crystal violet. Colonies consisting of more than 50 cells were scored.

Proliferation assay

Real-time cell proliferation assay was performed on E-Plate 16 using the RTCA DP instrument (Roche Applied Science). HONE1 cells were transfected with 0.75 nM, 1.5 nM or 3 nM ebv-miR-BART7 mimics (Qiagen) or negative control siRNA (Qiagen) using Hiperfect transfection reagent (Qiagen). After 24 hours, the transfected cells were transferred to a fresh medium and were irradiated at a single dose of 8 Gy; the cell prolifer-

ation rate was monitored continuously for 63 hours.

Apoptotic assays

Cell apoptosis was detected by Annexin V staining using Cytomics™ FC 500 (Beckman Coulter). HONE1 cells were transfected with 3 nM ebv-miR-BART7 mimics (Qiagen) or negative control siRNA (Qiagen) using Hiperfect transfection reagent (Qiagen). Twenty-four hours after transfection, the cells were irradiated at a single dose of 2, 4, 6 or 8 Gy. The irradiated cells were harvested and resuspended in Annexin-binding buffer (10 mM HEPES, 140 mM NaCl and 2.5 mM CaCl₂, pH 7.4) and stained with fluorescein isothiocyanate (FITC)-labelled Annexin V (Life Technologies™).

H2AX phosphorylation

Detection and quantification of phosphorylated H2AX (γH2AX) was performed according to the published protocol¹³. HONE1 cells were transfected with 3 nM ebv-miR-BART7 mimics (Qiagen) or negative control siRNA (Qiagen) using Hiperfect transfection reagent (Qiagen). Twenty-four hours after transfection, the cells were irradiated at a single dose of 2, 4, 6 or 8 Gy. The irradiated cells were stained with rabbit polyclonal anti-γH2AX antibodies (Abcam) and goat anti-rabbit immunoglobulin G-FITC conjugate (Life Technologies™). DAPI (Life Technologies™) and Alexa Fluor® 635 phalloidin (Life Technologies™) were used to stain the nucleus and F-actin. The number of γH2AX foci in the cells was counted using a fluorescent microscope.

Acridine orange (AO) staining

AO was used to detect cell autophagy after cell irradiation. Autophagy is characterised by the formation of acidic vesicular organelles (AVO). The AO-stained AVOs appear red. The cytoplasm and nucleolus appear as bright green and dim red, respectively¹⁴. After irradiation treatment, the cells were stained with 1 µg/ml

Licensee OA Publishing London 2013. Creative Commons Attribution Licence (CC-BY)

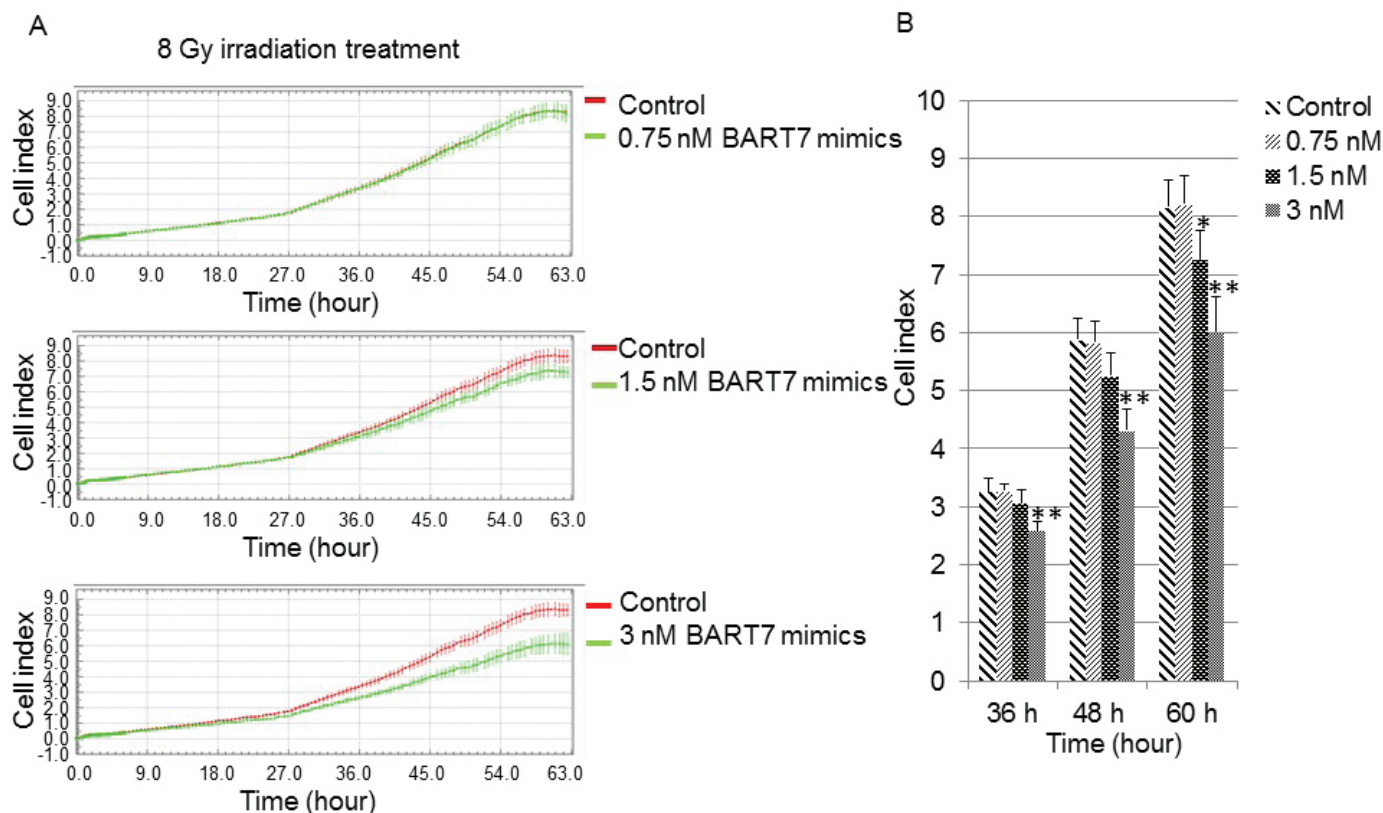


Figure 3: HONE1 cells transfected with ebv-miR-BART7 mimics exhibited a suppressed proliferation rate in comparison with HONE1 cells transfected with the negative control upon irradiation exposure. HONE1 cells were transfected with 0.75 nM, 1.5 nM or 3 nM ebv-miR-BART7 mimics or the negative control. Then, the cells were seeded on E-Plate 16 of the RTCA DP instrument. After 24 hours, cells were irradiated at a single dose of 8 Gy. (A) Cell proliferation was continuously monitored for 63 hours. (B) Cell proliferation at three time points (36 h, 48 h and 60 h). The assay was performed in triplicate. Bars indicate standard deviation, * $p < 0.05$ and ** $p < 0.01$ by Student's t-test.

AO (Sigma-Aldrich) and monitored using a fluorescent microscope.

Zebrafish NPC xenograft development and irradiation assays

In vivo radiation sensitivity was examined with the use of a zebrafish model according to a previously published protocol^{15,16}. A wild-type zebrafish strain was used to develop the NPC xenograft. The study was approved by the Committee on the Use of Live Animals in Teaching and Research at The University of Hong Kong (CULATR 2939-13). The zebrafish was kept at 28.5°C with 14/10 hour day-night cycle. The 48-hpf zebrafish embryos were anesthetised with tricaine (Sigma-Aldrich) before microinjection, under a dissecting light microscope (SMZ1000, Nikon). HONE1 cells transfected with 3 nM

ebv-miR-BART7 mimics (Qiagen) or control siRNA (Qiagen) were stained with DiO (Life Technologies™) before microinjection. The embryos were incubated in the zebrafish E3 embryo medium for 24 h before irradiation. Irradiation of the zebrafish embryos was performed with Gammacell® 3000 Elansystem (Best Theratronics Ltd.). Microscopic inspection was performed using an inverted microscope (CKX41, Olympus). The fluorescence signal was quantified using ImageJ¹⁷. The fluorescence signal of HONE1 cells transfected with the ebv-miR-BART7 mimics was normalised to that of HONE1 cells transfected with the negative control.

Statistical analysis

Statistical analysis was performed using the SPSS v16.0 (SPSS, Chicago,

Illinois, USA). Data are expressed as mean \pm standard deviation. All the tests were two-sided. A p value of <0.05 was considered statistical significant.

Results

Relative ebv-miR-BART7 expression level in tissue samples from patients with primary NPC, recurrent NPC and healthy controls

Ebv-miR-BART7 was detectable in all primary (42/42) and recurrent NPC tissues (29/29). In normal nasopharyngeal tissues, ebv-miR-BART7 was detected in 28/29 (97%) tissue samples. For the paired normal nasopharyngeal tissues obtained from the recurrent NPC patients, ebv-miR-BART7 was detected in 28/29 (97%) tissue samples.

Licensee OA Publishing London 2013. Creative Commons Attribution Licence (CC-BY)

In terms of quantity, levels of tissue ebv-miR-BART7 were significantly higher in primary cancer tissues as compared with the corresponding control tissues (Figure 1A). When we compared the ebv-miR-BART7 expression level between primary NPC, recurrent NPC and normal nasopharyngeal tissues obtained from different individuals, the ebv-miR-BART7 expression level was significantly higher in primary NPC tissues ($p < 0.001$, Mann-Whitney U test) and recurrent NPC tissues ($p < 0.001$, Mann-Whitney U test). In addition, primary NPC tissues had a significantly higher expression level of ebv-miR-BART7 as compared with the recurrent NPC tissues ($p < 0.001$, Mann-Whitney U test); for the recurrent NPC cases, paired normal tissues of the same individuals were available

(Figure 1B). When we compared the recurrent NPC tissues with the paired normal tissues, significantly higher levels of tissue ebv-miR-BART7 were observed ($p = 0.005$, Wilcoxon signed-rank test). In addition, we noticed that the normal tissues of recurrent NPC patients had a significantly higher level of ebv-miR-BART7 (Figure 1B) in comparison with the normal tissues obtained from the normal individuals (Figure 1A) ($p < 0.001$, Mann-Whitney U test).

Expression of ebv-miR-BART7 reduced the colony formation ability after radiation treatment

Without radiation treatment, ectopic expression of ebv-miR-BART7 in HONE1 cells had no significant effects on the colony formation ability. After radiation treatment, a dose-

dependent decrease in the number of colonies was observed. Significant reduction in the number of HONE1 colonies was observed when the cells were exposed to 2–8 Gy radiation (Figure 2).

Decreased proliferation rate in ebv-miR-BART7-expressing cells after radiation treatment

After radiation treatment, the proliferation of ebv-miR-BART7-expressing HONE1 cells was monitored continuously (Figure 3). At low ebv-miR-BART7 concentration (0.75 nM), no significant change in the proliferation rate was observed after radiation treatment. In comparison, when the ectopic expression level was increased from 0.75 nM to 1.5 and 3 nM, significant reduction in cell proliferation rate was observed when the cells were irradiated at a single dose of 8 Gy.

Expression of ebv-miR-BART7 promoted radiation-induced apoptosis in HONE1 cells

As shown in Figure 4, radiation treatment induced apoptosis in both control and ebv-miR-BART7-expressing cells in a dose-dependent manner. Without radiation treatment, ectopic ebv-miR-BART7 expression did not affect the apoptosis rate in the HONE1 cells. Significant increase in the apoptotic population was observed when the ebv-miR-BART7-expressing cells were exposed to radiation at 2–8 Gy.

Ectopic ebv-miR-BART7 expression enhanced the formation of γ H2AX foci in HONE1 cells upon irradiation treatment

To assess the effects of ebv-miR-BART7 on radiation-induced DNA double-strand break, we detected the formation of γ H2AX foci in HONE1 cells after irradiation treatment. Irradiation treatment resulted in the formation of γ H2AX foci in a dose-dependent manner in both control and ebv-miR-BART7-expressing cells (Figure 5). Forced ebv-miR-BART7

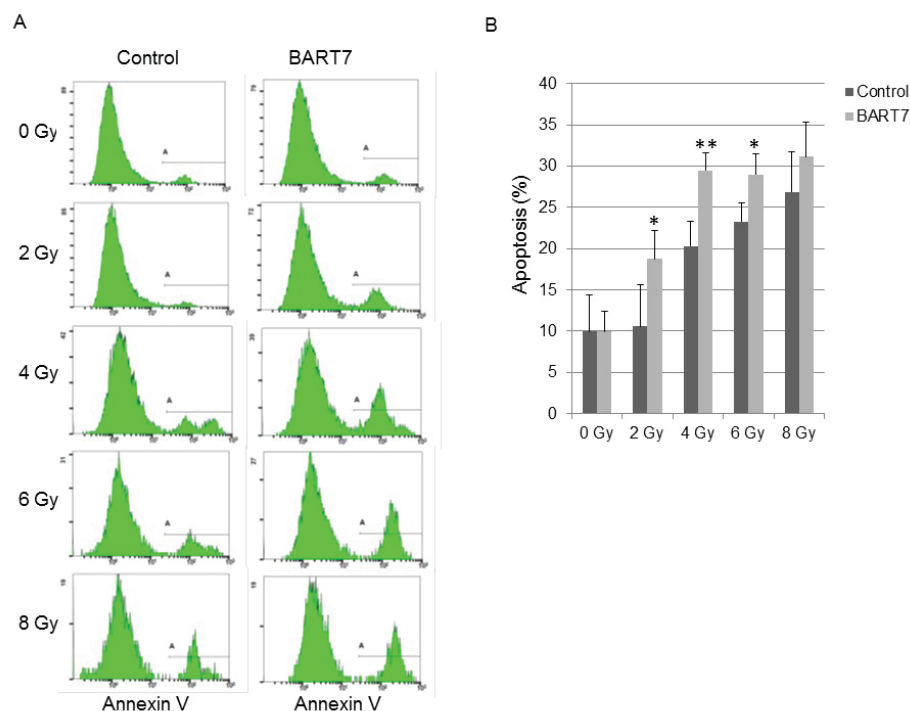


Figure 4: Ebv-miR-BART7 promoted irradiation-induced apoptosis in HONE1 cells. HONE1 cells were transfected with 3 nM ebv-miR-BART7 mimics or the negative control. After 24 hours, cells were irradiated at a single dose of 2, 4, 6 or 8 Gy. The irradiated cells were stained by FITC-labelled Annexin V and analysed by flow cytometry. (A) Representative pictures showing apoptosis of HONE1 cells after radiation treatment. (B) Statistical analysis of apoptosis of HONE1 cells after radiation treatment. The assay was performed in four-replicate. Bars indicate standard deviation, * $p < 0.05$ and ** $p < 0.01$ by Student's t-test.

Licensee OA Publishing London 2013. Creative Commons Attribution Licence (CC-BY)

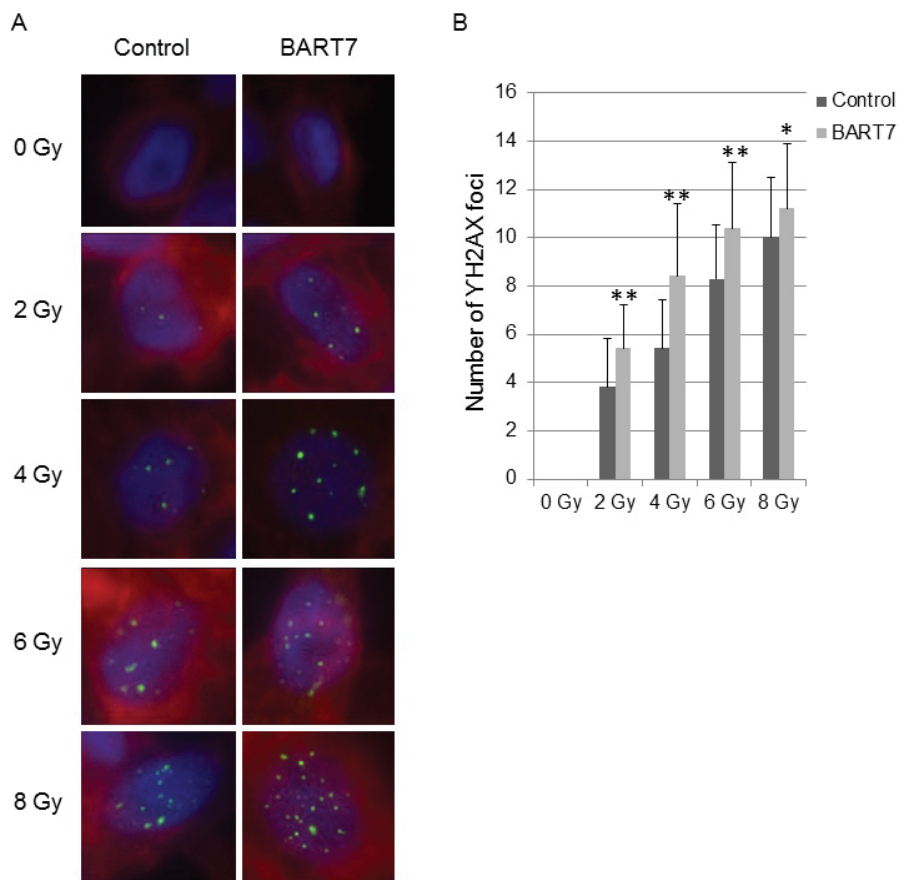


Figure 5: Ebv-miR-BART7 increased the formation of γ H2AX foci in HONE1 cells upon irradiation treatment. HONE1 cells were transfected with 3 nM ebv-miR-BART7 mimics or negative control siRNA. Twenty-four hours after transfection, the cells were irradiated at a single dose of 2, 4, 6 or 8 Gy. The irradiated cells were fixed and incubated with rabbit polyclonal anti- γ H2AX antibodies. DAPI and Alexa Fluor® 635 phalloidin were used to stain the nucleus and F-actin. (A) Representative pictures showing the formation of γ H2AX foci in HONE1 cells after radiation treatment. (B) Statistical analysis of the number of γ H2AX foci in cells. Bars indicate standard deviation, n = 50, * p < 0.05 and ** p < 0.01 by Student's t-test.

expression elevated the number of γ H2AX foci by 42.4%, 55.2%, 25.0% and 12.0% upon radiation treatment at the dose of 2, 4, 6 and 8 Gy, respectively (Figure 5).

Ectopic ebv-miR-BART7 expression promotes radiation-induced autophagy in HONE1 cells

Prominent changes in cell morphology were observed when the HONE1 cells were exposed to radiation stress. Increase in the number of cells entering autophagy was observed when the radiation dose increased from 2 Gy to 8 Gy. In the control

sample, cells filled with AVO were detected when the cells were exposed to radiation of 6 Gy or above. In ebv-miR-BART7-expressing cells, the AVO-filled cells appeared when the cells were exposed to 4 Gy (Figure 6).

ebv-miR-BART7 enhanced radiosensitivity of HONE1 cells in an *in vivo* zebrafish model

We used a zebrafish model to evaluate the effects of ebv-miR-BART7 expression on radiosensitivity of HONE1 cells *in vivo*. Forced expression of ebv-miR-BART7 resulted in the reduction of the fluorescence signal after radiation

treatment (Figure 7). At 2 Gy and 6 Gy, the fluorescence signal of ebv-miR-BART7-expressing cells was reduced by 30.3% and 38.9%, respectively, in comparison with the control. At 4 Gy, forced expression of ebv-miR-BART7 significantly reduced the fluorescence signal of HONE1 cells by 86.9% in the zebrafish model (Figure 7).

Discussion

The EBV genome contains 2 major clusters (BHRF1 and BART clusters) coding for 25 precursors and 44 mature viral-encoded miRNAs. In our preliminary study, we identified that ebv-miR-BART7 is a potent oncogene in NPC cells. Ebv-miR-BART7 is a viral-encoded miRNA that is highly expressed in NPC cells infected with EBV latently. Mature ebv-miR-BART7 (MIMAT0003416) is a single-stranded molecule containing 22 nucleotides (5'-CAUCAUAGUC-CAGUGUCCAGGG-3') with unknown functions. Ebv-miR-BART7 has gained much attention as its expression level is relatively high in comparison with other EBV-encoded miRNAs in EBV-infected cell lines⁹. In comparison with other BART members, expression levels of ebv-miR-BART7 in the host cell increases exponentially after EBV infection⁹. In 2010, Chen et al. observed that ebv-miR-BART7 expression was significantly upregulated in human NPC tissues¹⁸. Later, it was reported that circulating ebv-miR-BART7 was detected in the peripheral blood of NPC patients¹⁰. In this study, we first measured the expression of ebv-miR-BART7 in nasopharyngeal tissues. We observed that ebv-miR-BART7 could be detected in all the tissue samples and was differentially expressed. Both primary and recurrent NPC tissues had significantly high ebv-miR-BART7 levels in comparison with the normal controls. The high expression level of ebv-miR-BART7 in primary and recurrent NPC tissues suggested that ebv-miR-BART7 plays an important role in the development of the disease.

Licensee OA Publishing London 2013. Creative Commons Attribution Licence (CC-BY)

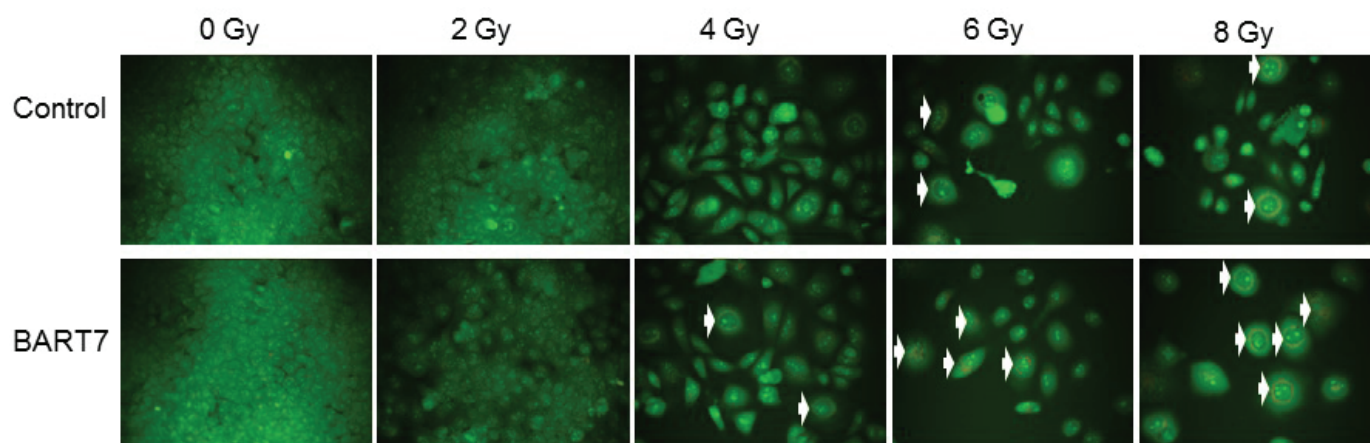


Figure 6: Representative pictures showed that ebv-miR-BART7 elevated radiation-induced autophagy in HONE1 cells. HONE1 cells were transfected with 3 nM ebv-miR-BART7 mimics or the negative control. Twenty-four hours after transfection, the cells were irradiated at a single dose of 2, 4, 6 or 8 Gy. The irradiated cells were stained with AO. Arrows indicate the staining of AVOs.

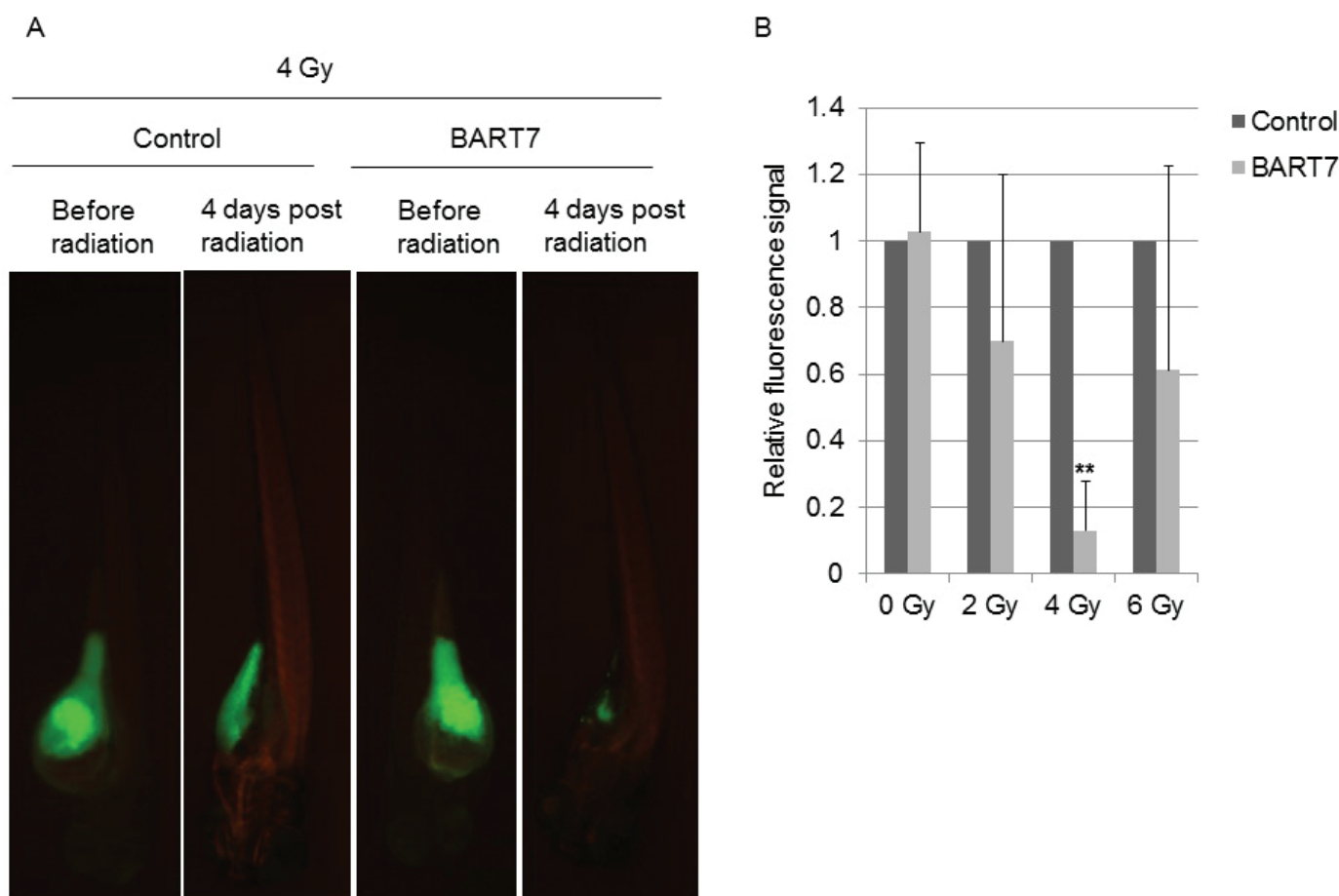


Figure 7: Ebv-miR-BART7 enhanced radiosensitivity of HONE1 cells in an *in vivo* zebrafish model. HONE1 cells transfected with ebv-miR-BART7 mimics or negative control siRNA were stained with DiO and microinjected into 48-hpf zebrafish embryos. Zebrafish embryos were subjected to irradiation 24 hours after microinjection. The fluorescence signal was determined before and 4 days after irradiation treatment. The fluorescence signal of HONE1 cells transfected with ebv-miR-BART7 mimics was normalised to that of HONE1 cells transfected with the negative control. (A) Representative pictures showing fluorescence signal of HONE1 cells in zebrafish embryos before and after irradiation treatment. (B) Statistical analysis of the relative fluorescence signal of HONE1 cells in zebrafish embryos upon irradiation treatment. Bars indicate standard deviation, $n = 5$, $**p < 0.01$ by Student's t-test.

Licensee OA Publishing London 2013. Creative Commons Attribution Licence (CC-BY)

FOR CITATION PURPOSES: Chan YWJ, Gao W, Li ZHJ, Ho WK, Wong TS. Expression of Epstein-Barr virus-encoded BamH1-a rightward transcript 7 microRNA in nasopharyngeal carcinoma cells modulates the responsiveness to irradiation treatment. *Head Neck Oncol.* 2013 Mar 06;5(3):34.



When we compared primary and recurrent NPC alone, we noticed that patients with recurrent NPC had a notably lower ebv-miR-BART7 level. Early recurrent NPC patients are usually treated with surgery, as a second course of radiation may damage the brainstem, the optic apparatus and the temporal lobes adjacent to the tumours, resulting in long-term side effects¹⁹. More importantly, the recurrent NPC tissue may have developed radiation resistance during the first course of radiation or may have developed from the intrinsically radiation-resistant clone which escaped initial radiotherapy²⁰. In general, patients with recurrent disease at the nasopharynx and/or neck nodes after radiotherapy are considered radioresistant patients⁶. If high ebv-miR-BART7 is a contributing factor to the high radiation sensitivity of primary NPC, cancer cells with low ebv-miR-BART7 might have the chance to escape from the first radiation treatment, leading to the development of recurrent disease. As the recurrent NPC patients did not receive radiation treatment again, we could not validate the suggested association on radiation sensitivity/resistance with the use of tissue samples. To examine the response of the NPC cells to ionising radiation, we therefore generated the ebv-miR-BART7-expressing model with the use of a NPC cell line. Based on these observations, we suggest that the expression of ebv-miR-BART7 is associated with primary NPC and is linked to the responsiveness of NPC cells to irradiation treatment. Further studies are warranted to confirm whether ebv-miR-BART7 could be used as a therapeutic biomarker to monitor the outcome of radiation-treated NPC patients.

Abbreviations list

AO, acridine orange; AVO, acidic vesicular organelles; EBV, Epstein-

Barr virus; ebv-miR-BART7, Epstein-Barr virus-encoded BamH1—a rightward transcript 7 microRNA; FITC, fluorescein isothiocyanate; miRNA, microRNA; NPC, nasopharyngeal carcinoma; SCC, squamous cell carcinoma; siRNA, small interfering RNA.

Acknowledgement

This study was supported by Seed Funding of Basic Research and Hong Kong Area of Excellent Scheme, Hong Kong UGC, Hong Kong.

References

1. Wei WI, Sham JS. Nasopharyngeal carcinoma. *Lancet*. 2005 Jun;365(9476):2041–54.
2. Niedobitek G. Epstein-Barr virus infection in the pathogenesis of nasopharyngeal carcinoma. *Mol Pathol*. 2000 Oct;53(5):248–54.
3. Wei KR, Xu Y, Liu J, Zhang WJ, Liang ZH. Histopathological classification of nasopharyngeal carcinoma. *Asian Pac J Cancer Prev*. 2011;12(5):1141–7.
4. DeNittis AS, Liu L, Rosenthal DI, Machtay M. Nasopharyngeal carcinoma treated with external radiotherapy, brachytherapy, and concurrent/adjuvant chemotherapy. *Am J Clin Oncol*. 2002 Feb;25(1):93–5.
5. Mould RF, Tai TH. Nasopharyngeal carcinoma: treatments and outcomes in the 20th century. *Br J Radiol*. 2002 Apr;75(892):307–39.
6. Feng XP, Yi H, Li MY, Li XH, Yi B, Zhang PF, et al. Identification of biomarkers for predicting nasopharyngeal carcinoma response to radiotherapy by proteomics. *Cancer Res*. 2010 May;70(9):3450–62.
7. Pan Y, Zhang Q, Atsaves V, Yang H, Claret FX. Suppression of Jab1/Csn5 induces radio- and chemo-sensitivity in nasopharyngeal carcinoma through changes to the DNA damage and repair pathways. *Oncogene*. 2012 Jul.
8. Pratt ZL, Kuzembayeva M, Sengupta S, Sugden B. The microRNAs of Epstein-Barr Virus are expressed at dramatically differing levels among cell lines. *Virology*. 2009 Apr;386(2):387–97.
9. Rana TM. Illuminating the silence: understanding the structure and function of small RNAs. *Nat Rev Mol Cell Biol*. 2007 Jan;8(1):23–36.
10. Chan JY, Gao W, Ho WK, Wei WI, Wong TS. Overexpression of Epstein-Barr virus-encoded microRNA-BART7 in undifferentiated nasopharyngeal carcinoma. *Anti-cancer Res*. 2012 Aug;32(8):3201–10.
11. Choy EY, Siu KL, Kok KH, Lung RW, Tsang CM, To KF, et al. An Epstein-Barr virus-encoded microRNA targets PUMA to promote host cell survival. *J Exp Med*. 2008 Oct;205(11):2551–60.
12. Glaser R, Zhang HY, Yao KT, Zhu HC, Wang FX, Li GY, et al. Two epithelial tumour cell lines (HNE-1 and HONE-1) latently infected with Epstein-Barr virus that were derived from nasopharyngeal carcinomas. *Proc Natl Acad Sci U S A*. 1989 Dec;86(23):9524–8.
13. MacPhail SH, Banáth JP, Yu TY, Chu EH, Lambur H, Olive PL. Expression of phosphorylated histone H2AX in cultured cell lines following exposure to X-rays. *Int J Radiat Biol*. 2003 May;79(5):351–8.
14. Traganos F, Darzynkiewicz Z. Lyso-somal proton pump activity: supravital cell staining with acridine orange differentiates leukocyte subpopulations. *Methods Cell Biol*. 1994;41:185–94.
15. Nicoli S, Presta M. The zebrafish/tumour xenograft angiogenesis assay. *Nat Protoc*. 2007;2(11):2918–23.
16. Geiger GA, Parker SE, Beothy AP, Tucker JA, Mullins MC, Kao GD. Zebrafish as a “biosensor”? Effects of ionizing radiation and amifostine on embryonic viability and development. *Cancer Res*. 2006 Aug;66(16):8172–81.
17. Collins TJ. ImageJ for microscopy. *Biotechniques*. 2007 Jul;43(1 Suppl):25–30.
18. Chen SJ, Chen GH, Chen YH, Liu CY, Chang KP, Chang YS, et al. Characterization of Epstein-Barr virus miRNAome in nasopharyngeal carcinoma by deep sequencing. *PLoS One*. 2010 Sep;5(9):e12745.
19. Chen C, Fee W, Chen J, Chan C, Khong B, Hara W, et al. Salvage treatment for locally recurrent nasopharyngeal carcinoma (NPC). *Am J Clin Oncol*. 2012 Dec.
20. Suárez C, Rodrigo JP, Rinaldo A, Langendijk JA, Shaha AR, Ferlito A. Current treatment options for recurrent nasopharyngeal cancer. *Eur Arch Otorhinolaryngol*. 2010 Dec;267(12):1811–24.

Licensee OA Publishing London 2013. Creative Commons Attribution Licence (CC-BY)

FOR CITATION PURPOSES: Chan YWJ, Gao W, Li ZHJ, Ho WK, Wong TS. Expression of Epstein-Barr virus-encoded BamH1-a rightward transcript 7 microRNA in nasopharyngeal carcinoma cells modulates the responsiveness to irradiation treatment. *Head Neck Oncol*. 2013 Mar 06;5(3):34.